RSC Advances

ROYAL SOCIETY OF CHEMISTRY

www.rsc.org/advances

A novel and effective method to fabricate flame retardant and smoke suppressed flexible polyurethane foam

Ying Pan[1], Jing Zhan [1,2], Haifeng Pan[1,3], Wei Wang[1,3], Hua Ge[1], Lei Song[1*], Yuan Hu[1,3*]

1. State Key Laboratory of Fire Science, University of Science and Technology of China, Hefei, Anhui 230026, PR China
2. School of Civil Engineering and Environmental Engineering, Anhui Xinhua University, Hefei, Anhui 230088, PR China
3. Suzhou Key Laboratory of Urban Public Safety, Suzhou Institute for Advanced Study, University of Science and Technology of China, Suzhou, Jiangsu 215123, PR China

Abstract: In the present work, chitosan and magnesium hydroxide (MH) were successfully deposited on the surface of flexible polyurethane foam (FPUF). Due to the strong interaction, the coated foam with 10.3 wt% weight-gain could be prepared by constructing one chitosan layer and one MH layer. Scanning electron microscopy images showed that this coating covered continuously on the substrate. The combustion properties of FPUF were investigated by cone calorimeter and smoke density tests, and the gases released during the thermal degradation process were monitored by thermal gravimetric-Fourier transform infrared spectrometry. It's found

* Corresponding author. Tel/Fax: +86 551 63601664.
E-mail address: yuanhu@ustc.edu.cn (Y. Hu)

that the FPUF with a chitosan/MH coating kept its shape and released less black smoke after being exposed to a butane flame for 10s, while the pure foam was consumed completely. The cone calorimeter test data indicated that a reduction in the peak heat release rate of the foam with 10.3 wt% weight-gain achieved 52.6% relative to pure foam. Remarkably, the smoke density test results showed that the coating can significantly suppress the smoke production of FPUF. Moreover, the evolved gas products of FPUF during the thermal decomposition were effectively decreased after being covered with the hybrid coating.

Keywords: Magnesium hydroxide; Coating; Flexible polyurethane foam; Flame retardancy; Smoke suppression

1. Introduction:

As a kind of polymer material, flexible polyurethane foams (FPUF) have a wide range of applications, including furniture, construction and automotive fields [1-3] due to their good cushioning, high durability, good thermal and acoustic insulation properties, resistance to chemicals, low price and low density. [4-6] However, FPUF readily ignites and burns rapidly with a high rate of heat release and evolution of wide range of combustion products like, smoke and toxic gases, such as hydrocarbons, isocyanates, etc. [7]. Many literatures have reported flame retardant studies and analysis of hazardous components about FPUF. [8-10] Most of the earlier studies focused on the effect of flame retardants that include phosphorus[3, 11], nitrogen[12] and halogen[13] based compounds on FPUF. The use of most commonly used halogen based flame retardant additives for FPUF, such as Tris(2-chloroethyl) phosphate (TCEP),

Tris(1,3-dichloroisopropyl) phosphate (TDCPP) and Tris(1-chloro-2-propyl) phosphate (TCPP) is currently restricted because of their potential toxicity and environment problems arising from FPUF's storage, transportation and combustion.[14, 15] Therefore there is a great need to develop environmental friendly flame retardants to replace these halogen based compounds. Over past decade several kinds of organophosphorus compounds have been reported as flame retardant additives for FPUF. A series of organophosphorus compounds (phosphonates, phosphates and phosphoramidates) were synthesized and incorporated into the FPUF by Shuyu Liang et al.[2] With 5 wt% addition of these additives, small reduction was resulted in peak heat release. Considerable restrictions have been put on these traditional flame retardants, due to the release of highly toxic combustion products resulting in environmental contaminations and hazards. [16, 17] Therefore, much attention has been attracted by new environment-friendly and highly effective flame retardant and smoke suppression technologies. This fact is attested by intensive research activity and ever-growing number of publications in this field.

Since Grunlan et al. [18] first used Layer-by-Layer (LbL) assembly technique to produce a flame retardant coating on fabric in 2009, this technique has been widely exploited to lower the flammability of polymers and many researches indicate that this technique is quite efficient for FPUF to improve its fire resistance. [19-21] Lots of materials, such as polyelectrolytes, nanoparticles and micelles can be utilized to form the multilayers on the substrates and endow them with multifunctional properties. [22] For fabricating the LbL assembled and flame retardant coatings, polyelectrolytes and

nanoparticles are used simultaneously or independently. Grunlan et al. prepared an effective flame retardant coating comprised of positively charged chitosan and anionic poly(vinyl sulfonic acid sodium salt) (PVS) on FPUF using LbL assembly technique. [23] The FPUF coated with 10 chitosan-PVS bilayers has a 52% reduction in the peak heat release rate compared with a uncoated one. A three-component coating comprised of sodium montmorillonite, poly(allylamine hydrochloride) and poly(sodium phosphate) (PSP) were constructed via LbL assembly. [24] This coating completely shut down melt-dripping and reduced the heat release of FPUF when exposed to direct flame, which is due to a synergistic interaction between PSP and thermally shielding clay platelets in the condensed phase. The LbL assembly coatings show excellent fire resistance. However LbL procedure requires multiple steps and is time-consuming.

On the other hand, magnesium hydroxide (MH) is a widely used metal hydroxide for flame retardant [25-27] by liberation of water molecule (cooling effect) on its decomposition [$Mg(OH)_2 \rightarrow MgO + H_2O$ ΔH = 328 cal/g] [28] and many investigations have demonstrated that MH is a non-toxic and good smoke-suppressing halogen-free flame retardant. [29] However, it has a fatal disadvantage that more than 50% MH loading is required to meet fire resistance properties, which would dramatically destroy the mechanical requirement of the polymer composites. [25]

In the present work, a novel and effective method for constructing a fire resistant coating on the surface of FPUF was proposed. The coating was made of one chitosan layer and one MH layer, as shown in Fig. 1. SEM images in Fig. 3 indicated that the

coatings were fully covered on the surface of FPUFs. After the sample was covered with this coating, the peak heat release rate (PHRR) and smoke production were reduced. Above mentioned results of present investigation reveal the fact that this study has a strong potential to industrial usage for flame retardant and smoke suppressed FPUF.

2. Experimental section

2.1 Materials

FPUF (DW30) was obtained from Jiangsu Lvyuan New Material Co., Ltd. Nano-MH was purchased from Henan Tianlong flame retardant material Co., Ltd. Poly(acrylic acid) (PAA, Mw~3000), chitosan (viscosity: 50-800 mPa •s, degree of deacetylation 80-95%), hydrochloric acid (HCl 36-38%) and sodium hydroxide were provided by Sinopharm Chemical Reagent Co., Ltd. 0.5 wt% chitosan and 0.1 wt% PAA aqueous solution was magnetically stirred and the pH was adjusted to 5 and 1 respectively wih 1 M HCl until it was completely dissolved. Nano-MH suspension was prepared by adding nano-MH to deionized water and pH was adjusted to 10, then the mixture was stirred and sonicated for 24 h.

2.2 The coating deposition

FPUF was firstly immersed in the 0.1 wt % PAA solution for 5 min to obtain negatively charged sample. [30] Then the treated FPUF was successively immersed in the solutions of chitosan and MH for 2 min, each. Before MH was deposited on the surface of FPUF, the weight-gain of FPUF modified by PAA and chitosan is 0.5 wt%.

Each time after soaking in solutions, the foam was washed in the deionized water for 2 min. As shown in Fig. 1, with the once immersion of FPUF, most of the MH in the solution deposited on the surface of chitosan coated FPUF. When 10g FPUFs immersed into the MH suspensions, these suspensions contained 0.5g and 1g MH respectively so that the MH weight-gain of the FPUFs could theoretically achieve 5 wt% and 10wt%, respectively. Actually after being coated with one chitosan layer and one MH layer, the weight-gain were 4.9 wt% and 10.3 wt%. This dramatic absorption of coating was due to the easy agglomeration of nano-MH and electrostatic interaction between chitosan and MH. [31, 32] In this work, we denote briefly the coated FPUF with 4.9 wt% and 10.3 wt% weight-gain as FPUF-1 and FPUF-2, respectively.

3. Measurements.

Attenuated total reflection Fourier transform infrared (ATR-FTIR) spectra with the frequency region from 4000 to 400 cm^{-1} were recorded by a Nicolet 6700 spectrometer (Thermo-Nicolet) using 32 scans.

The morphologies of control and coated FPU foams coated with a gold layer in advance were observed using scanning electron microscopy (SEM, FEI, Sirion200).

Limiting oxygen index (LOI) tests was performed at room temperature according to ISO 4589-2 using a HC-2C oxygen index instrument, and the size of the specimen was 150 × 10 × 10 mm^3 (length × width × thickness).

Pure and coated foams were exposed to the direct flame of a butane torch (CFZ-2-type instrument, Jiangning Analysis Instrument Company, China) for 10s to

provide a visual evaluation of coating effectiveness.

The combustion test was performed on the cone calorimeter (Fire Testing Technology, UK) tests according to ISO 5660 standard procedures, with 100 × 100 × 25 mm^3 specimens. Each specimen was exposed horizontally to 50 kW/m^2 external heat flux. Meanwhile, the cone data were based on three repeats.

The optical density was determined by smoke density test machine (JQMY-2, Jianqiao Co, China). For the decomposition model, the closed chamber is used according to ISO 5659-2. Samples of 75 × 75 × 25 mm^3 are positioned horizontally underneath a conical heater and exposed to an irradiance of 25 kW m^{-2} with an additional pilot burner. Three repeats were done in the smoke density test.

Thermogravimetric analysis- Fourier transform infrared spectrometry (TG-FTIR) of the samples was performed using a TGA Q5000 IR thermogravimetric analyzer that was interfaced to the Nicolet 6700 FTIR spectrophotometer through a Thermo-Nicolet TGA special connector.

4. Result and Discussion

4.1 Coating Growth and Microstructure

To evaluate the growth of coating on the FPUF, ATR-FTIR spectroscopy was used to detect the characteristic groups on the surface of FPUF. The ATR-FTIR spectra of the pure and coated FPUFs are shown in the Fig. 2. The peak at 1100 cm^{-1} is ascribed to the C-O-C stretching vibration of polyurethane foam. [33] Compared with the pure FPUF, the absorbance intensity of the C-O-C peak gradually becomes weak,

demonstrating that the coatings are successfully deposited on the substrate.

Fig. 3 shows the SEM images of the pure and coated FPUF. In Fig. 3a, it can be seen that the pure FPUF has a smooth surface. The SEM images of coated FPUFs in Fig. 3b and c show that the surfaces of FPUF-1 and FPUF-2 have been fully covered with the chitosan/MH. In order to characterize the roughness and thickness of coating, the view of coated FPUFs' fracture are shown in Fig. 3d and e. It is obvious that the coating on FPUF-2 is thicker and rougher than that of FPUF-1, which demonstrates that more MH have been absorbed on FPUF-2.

In order to quantitatively characterize the MH on the surface of the two samples, EDX spectra of pure and coated FPUFs are shown in Fig. 4 as a representation to monitor the element composition of samples. The Mg element is only detected in the coated FPUFs, indicating the presence of MH on the surface of FPUF-1 and FPUF-2. As weight-gain of the coating becomes higher, the atomic percent of Mg clearly increases. This result provides direct evidence to indicate the present of MH on the surface of coated FPUFs.

4.2 Flame Retardant properties of FPUFs

The flammability of FPUF was initially evaluated by holding the flame from a butane torch on the foam's surface for 10 s. The uncoated FPUF was ignited immediately, formed a melt pool, and completely consumed. As shown in Fig. 5a, it is obviously that the melt-dripping is serious and black smoke can be clearly seen during the combustion. In Fig. 5b and c, no melt-dripping appears and the flame is retarded obviously. Furthermore, the black smoke during combustion significantly reduces (see

Fig. 5 and video in Supplementary Information). The cross sections of FPUF-1 and FPUF-2 after combustion are shown in Fig. 5d and e. It is found that these char residues keep their original shape. This may be caused by the chitosan/MH coating can insulate the heat transformation and oxygen to protect the underlying polymeric substrate. Specifically there exist some unburned parts on char residue of FPUF-2. During the decomposition of MH, water vapor generates with heat absorption of 1300 J/g, which lowered the temperature of FPUF's surface to prevent fire transmission (cooling effect). [34]

The flame retardant properties of FPUFs were evaluated by LOI test and cone calorimeter. In the LOI test, after being covered with chitosan/MH coating, the LOI value of FPUF can increases from 17.5 to 20.5. Moreover the LOI value of FPUFs with 20 wt% and 30 wt% weight-gain are also 20.5. It can be concluded that the further absorption of MH does not contribute the LOI value. The cone calorimeter, based on the oxygen consumption principle, has been widely used to investigate the combustion behaviors of materials. Some important information such as heat release rate (HRR), total heat release (THR) are recorded to evaluate the fire behaviors of material in real fires. [35] Fig. 6 shows the HRR and THR curves of the pure and coated FPUFs and the related cone data are listed in Table 1.The combustion of pure FPUF is accompanied by significant change in volume, due to the collapse of the foam to low viscosity liquid. The first peak on the HRR curve is assigned to the collapse of the foam and the second stage corresponds to pool fire. [36] It can be seen that the pure FPUF burns fast after ignition and a sharp HRR peak appears with a peak heat release

rate (PHRR) of 736 kW/m^2. After being covered with 4.9 wt% weight gain coating, the PHRR of FPUF-1 decreases greatly, reaching 403 kW/m^2. Moreover a significant suppression in fire risk of FPUF-2 is observed, with the reduction in peak heat release rate of 52.6%, compared to the pure FPUF. This can be assigned to the inorganic coating can retard the heat and flammable gases transmission. However, the THR of FPUF-1 and FPUF-2 improve slightly, which suggests that in the cone test, the chitosan/MH coatings do not contribute carbonization process and the FPUFs burn fully.

Fig. 7 shows the photograph of specimens after cone calorimeter for pure FPUF, FPUF-1 and FPUF-2. It can be seen that pure FPUF left small amount of char residue, while the coated FPUFs form the white residues. These fragile white residues are supposed to be MgO. With the increasing of MH, the residue of FPUF-2 could maintain its original shape, while the residue of FPUF-1 collapsed. These char residues were characterized by FTIR and the spectra are shown in Fig. 8. The characteristic absorption peaks of the residue from coated foams are similar to that of MgO. Moreover, the color of the coated foams' residue is white, demonstrating that the residue of the coated foams mainly consists of MgO. From the spectra of MgO and residue of FPUF-1 and FPUF-2, it can be observed apparently that strong band at 426 cm^{-1} associate with the characteristic vibrational mode of symmetric MgO_6 octahedra of MgO. The absorption at 3453 cm^{-1} indicates that the presence of hydroxyl, which is probably due to the fact that the spectra are not recorded in situ and some readsorption water from the ambient atmosphere has occurred. The peaks in

the range of 1300- 1700 cm^{-1} also are related to hydroxyl groups.[37] The results above indicate that the FPUF matrix under the coating combust more sufficiently than the pristine FPUF under the continuous and strong radiative heat flux. This maybe can explain why the THR values of coated FPUF are higher than that of pure one.

4.3 Smoke suppression of FPUFs

The detailed information about the smoke production was characterized by smoke density test. [38] Fig. 9 shows the smoke density of pure FPUF, FPUF-1 and FPUF-2 during burning. It can be observed that the smoke production rate of pure FPUF is faster than that of FPUF-2. The smoke density of pure FPUF becomes stable after 150s and the plateau value is about 400, while the FPUF-2 presents a density peak of 305 at 265s. After covered with MH coating, the smoke density of foam significantly decreases. A smoke production model about the burning FPUF was built based on the literatures as shown in Fig. 10. [39] The smoke production of FPUF contains two parts: the first part, the thermal degradation products release from the condensed phase into the gas phase by breaking through the carbon layer. The second part, the gaseous degradation products grow into smoke aerosol. During the decomposition of MH coated FPUF, the heat is absorbed from FPUF matrix to increase intermolecular cross-linking reaction ratio and the active MgO from MH thermal decomposition promotes the FPUF carbonization to reduce the hydrocarbons and benzene release. The smoke nuclear and soot particles are reduced by the sorption of MgO. Because of the variety of effect from MH, the amount of the harmful volatiles is reduced. [40]

4.4 TG-FTIR analysis of pure FPUF and coated FPUF

TG-FTIR was used to analyze the gas products during the thermal degradation process of the materials. The FTIR spectra of volatilized pyrolysis product emitted from pure FPUF, FPUF-1 and FPUF-2 at the maximum evolution rate are shown in Fig. 11a. As shown in Fig. 11a, the absorption peaks of pyrolysis products of the pure FPUF are similar to those of FPUF-1 and FPUF-2, indicating that the existence of the coatings do not significantly change the thermal decomposition process of FPUF. Some of the volatilized pyrolysis products of FPUF can be detected by FTIR signals: the bands at 2930-2982 cm^{-1} are assigned to the aliphatic C-H bonding coming from various alkanes; the peak at 2150 cm^{-1} is ascribed to the stretching vibration of carbon monoxide; the characteristic peak at 1742 cm^{-1} is due to the absorbance of stretching vibration of C=O group; the peaks at 1378 and 1112 cm^{-1} correspond to the C-O bond arising from ethers.

In Fig. 11b-f, total and some specific volatilized products were selected to investigate, concluding hydrocarbons (2975 cm^{-1}), CO (2150 cm^{-1}), carbonyl compounds (1741cm^{-1}) and amide (1462 cm^{-1}). It can be seen that the absorbance intensities of pyrolysis products for FPUF-1 and FPUF-2 are lower than that for pure FPUF, especially hydrocarbons. Moreover, the pyrolysis products reduce with the addition of coating. As shown in Fig. 10, thermal degradation products of FPUF release from the condensed phase into the gas phase by breaking through the carbon layer. The reduced amount of these organic volatiles results in the inhibition of smoke due to that the organic volatiles may crack in to smaller hydrocarbon molecules and smoke particles, which can be further condensed or aggregated to form smoke.

Therefore, the decrease of smoke density can be observed in the smoke density test.

4.5 Bonding properties of the coating

In order to evaluate the bonding ability of the hybrid coatings on the surface, the coated foams were compressed to half of its original height for 100 times. The compressed FPUF-1 and FPUF-2 were denoted as FPUF-1c and FPUF-2c, respectively. After compression, the coated FPUF still maintain its original weight-gain and the PHRR of coated FPUFs improve slightly. As shown in Fig. 12, the second peaks of FPUF-1 and FPUF-2 nearly disappear, while the second peaks of FPUF-1c and FPUF-2c can be easily observed. It is known that the second stage corresponds to the pool fire, which means that generation of quickly released flammable gases would lead to the second, higher PHRR.[1] The coated foams after compression process, some defects generated on the hybrid coating. The coating can't insulate the heat and flammable gases effectively. Thus the second peak on HRR curves increase slightly after compression.

5. Conclusion

FPUF was successfully coated with chitosan and MH by LbL assembly technique. SEM images indicated that the FPUF-1 and FPUF-2 were fully covered with the coating. This MH containing coating flame retardant FPUF changed MH's original impression that of low efficiency of flame retardant. With 10.3 wt% chitosan/MH coating, the foam burned without melt-dripping and the black smoke was hard to observe when being ignited by a butane torch. The results of cone tests showed that the PHRR of FPUF-2 decreases 52.6% compared to the pristine foam, indicating a

significant suppression of fire risk. The smoke density test revealed that the smoke production of the FPUF with chitosan and MH coating obviously decreased during combustion process. Less gas was released from the coated foam during the TG-FTIR tests. Due to the cheap and environmental-friendly materials, simple preparation and excellent performance, this procedure has a strong potential to industrial usage for fabricating the flame retardant and smoke suppressed FPUF.

Acknowledgments

The work was financially supported by the National Basic Research Program of China (973 Program) (2014CB931804) and National Natural Science Foundation of China (No. 51473154 and 51303165).

Reference

1. R. H. Krämer, M. Zammarano, G. T. Linteris, U. W. Gedde and J. W. Gilman, *Polym Degrad Stab*, 2010, **95**, 1115-1122.
2. S. Liang, M. Neisius, H. Mispreuve, R. Naescher and S. Gaan, *Polym Degrad Stab*, 2012, **97**, 2428-2440.
3. A. Wolska, M. Goździkiewicz and J. Ryszkowska, *J Mater Sci*, 2012, **47**, 5627-5634.
4. M. Sultan, H. N. Bhatti, M. Zuber, I. A. Bhatti and M. A. Sheikh, *Carbohydr Polym*, 2011, **86**, 928-935.
5. H. Wang, E. Wang, Z. Liu, D. Gao, R. Yuan, L. Sun and Y. Zhu, *J Mater Chem A*, 2015, **3**, 266-273.

6. A. A. Nikkhah, H. Zilouei, A. Asadinezhad and A. Keshavarz, *Chem Eng J*, 2015, **262**, 278-285.

7. M. Boutin, J. Lesage, C. Ostiguy, J. Pauluhn and M. J. Bertrand, *J Anal Appl Pyrolysis* 2004, **71**, 791-802.

8. Y. Zhang, Z. Xia, H. Huang and H. Chen, *Polym Test*, 2009, **28**, 264-269.

9. D. K. Chattopadhyay and D. C. Webster, *Prog Polym Sci*, 2009, **34**, 1068-1133.

10. M. Berta, C. Lindsay, G. Pans and G. Camino, *Polym Degrad Stab*, 2006, **91**, 1179-1191.

11. C.-Q. Wang, F.-Y. Ge, J. Sun and Z.-S. Cai, *J Appl Polym Sci*, 2013, **130**, 916-926.

12. X.-L. Wang, K.-K. Yang and Y.-Z. Wang, *J Appl Polym Sci*, 2001, **82**, 276-282.

13. S. V. Levchik and E. D. Weil, *Polym Int*, 2004, **53**, 1585-1610.

14. S. Gaan, S. Liang, H. Mispreuve, H. Perler, R. Naescher and M. Neisius, *Polymer Degradation and Stability*, 2015, **113**, 180-188.

15. I. van der Veen and J. de Boer, *Chemosphere*, 2012, **88**, 1119-1153.

16. H. M. Stapleton, S. klosterhaus, S. Eagle, J. Fun, J. D. Meeker, A. Blum and T. F. Webster, *Environmental science & technology*, 2009, **43**, 7490-7495.

17. H. M. Stapleton, S. Klosterhaus, A. Keller, P. L. Ferguson, S. van Bergen, E. Cooper, T. F. Webster and A. Blum, *Environmental science & technology*, 2011, **45**, 5323-5331.

18. Y. C. Li, J. Schulz and J. C. Grunlan, *ACS applied materials & interfaces*, 2009, **1**, 2338-2347.

19. Y. S. Kim and R. Davis, *Thin Solid Films*, 2014, **550**, 184-189.

20. Y.-C. Li, Y. S. Kim, J. Shields and R. Davis, *Journal of Materials Chemistry A*, 2013, **1**, 12987.

21. Y. S. Kim, R. Harris and R. Davis, *ACS Macro Letters*, 2012, **1**, 820-824.

22. P. K. Deshmukh, K. P. Ramani, S. S. Singh, A. R. Tekade, V. K. Chatap, G. B. Patil and S. B. Bari, *J Controlled Release*, 2013, **166**, 294-306.

23. G. Laufer, C. Kirkland, A. B. Morgan and J. C. Grunlan, *ACS Macro Lett*, 2013, **2**, 361-365.

24. A. A. Cain, C. R. Nolen, Y.-C. Li, R. Davis and J. C. Grunlan, *Polym Degrad Stab*, 2013, **98**, 2645-2652.

25. Z. Wang, B. Qu, W. Fan and P. Huang, *J Appl Polym Sci*, 2001, **81**, 206-214.

26. U. Braun and B. Schartel, *Macromol Chem Phys*, 2004, **205**, 2185-2196.

27. L. Haurie, A. I. Fernández, J. I. Velasco, J. M. Chimenos, J.-M. Lopez Cuesta and F. Espiell, *Polym Degrad Stab*, 2007, **92**, 1082-1087.

28. M. Sain, S. H. Park, F. Suhara and S. Law, *Polym Degrad Stab*, 2004, **83**, 363-367.

29. M. Fu and B. Qu, *Polym Degrad Stab*, 2004, **85**, 633-639.

30. D. Patra, P. Vangal, A. A. Cain, C. Cho, O. Regev and J. C. Grunlan, *ACS applied materials & interfaces*, 2014, **6**, 16903-16908.

31. M. Liu, J. Xu, B. Cheng, W. Ho and J. Yu, *Applied Surface Science*, 2015, **332**,

121-129.

32. K. Tong, X. Song, G. Xiao and J. Yu, *Industrial & Engineering Chemistry Research*, 2014, **53**, 4755-4762.

33. Y. Liu, J. Ma, T. Wu, X. Wang, G. Huang, Y. Liu, H. Qiu, Y. Li, W. Wang and J. Gao, *ACS applied materials & interfaces*, 2013, **5**, 10018-10026.

34. J. Zhao, X. Zhang, R. Tu, C. Lu, X. He and W. Zhang, *Cellulose*, 2014, **21**, 1859-1872.

35. B. Wang, X. Wang, Y. Shi, G. Tang, Q. Tang, L. Song and Y. Hu, *Radiat Phys Chem*, 2012, **81**, 308-315.

36. X. Wang, Y.-T. Pan, J.-T. Wan and D.-Y. Wang, *RSC Adv*, 2014, **4**, 46164-46169.

37. F. Gu, S. F. Wang, M. K. Lü, W. G. Zou, G. J. Zhou, D. Xu and D. R. Yuan, *Journal of Crystal Growth*, 2004, **260**, 507-510.

38. X. Chen, Y. Jiang and C. Jiao, *Journal of hazardous materials*, 2014, **266**, 114-121.

39. Q. Xu, H. Zhai and G. Wang, *Fire and Mater*, 2015, **39**, 271-282.

40. T. Xu and X. Huang, *J Anal Appl Pyrolysis*, 2010, **87**, 217-223.

Table Captions:

Table 1 CONE results for the uncoated and coated FPUF.

Sample	LOI	TTI (s)	pHRR (kW/m^2)	THR (kJ/m^2)
FPUF	**17.5**	**5**	**736**	**19.3**
FPUF-1	**20.5**	**6**	**403**	**19.6**
FPUF-2	**20.5**	**5**	**349**	**20.2**

TTI: time to ignition; PHRR: peak heat release rate; THR: total heat release.

Figure captions:

Fig. 1. Schematic of construction of chitosan/MH coatings on the FPUF. The FPUF was first immersed in chitosan solution, then immersed in MH suspension.

Fig. 2. ATR-FTIR spectra of pure and coated FPUFs.

Fig. 3. SEM images of pure FPUF (a), FPUF-1 (b) and FPUF-2 (c).

Fig. 4. EDX spectra of the pure FPUF, FPUF-1 and FPUF-2.

Fig. 5. Photographs of 40s after ignition by holding the flame from a butane torch on the surfaces of pure FPUF (a), FPUF-1 (b) and FPUF-2 (c) for 10 s. Cross section images of FPUF-1 (d) and FPUF-2 (c)'s char residues after burning.

Fig. 6. Heat release rate (a) and total heat release (b) curves of pure and coated FPUFs.

Fig. 7. Photographs of pure FPUF (a), FPUF-1 (b) and FPUF-2 (c) after cone calorimeter.

Fig. 8. FTIR curves of uncoated and coated FPUF's char residue after CONE and MgO.

Fig. 9. Released smoke density of pure FPUF, FPUF-1 and FPUF-2 while burning under 25kW m^{-2} heat flux.

Fig. 10. Model of smoke generation from the burning coated FPUF.

Fig. 11. FTIR spectra of volatilized pyrolysis product emitted from pure FPUF, FPUF-1 and FPUF-2 at maximum evolution rate (a). Absorbance of pyrolysis products for pure FPUF, FPUF-1 and FPUF-2 vs time: (b) Total; (c) Hydrocarbons; (d) CO; (e) Carbonyl and (f) amide.

Fig. 12. Heat release rate curves of coated FPUF (FPUF-1 and FPUF-2) and coated FPUF after compression (FPUF-1c and FPUF-2c).

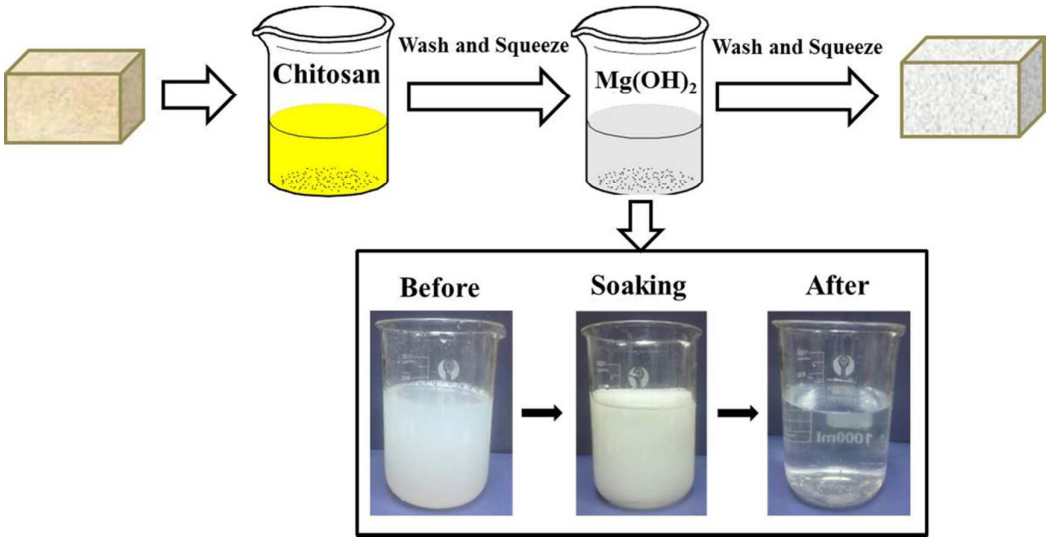

Fig. 1. Schematic of construction of chitosan/MH coatings on the FPUF. The FPUF was first immersed in chitosan solution, then immersed in MH suspension.

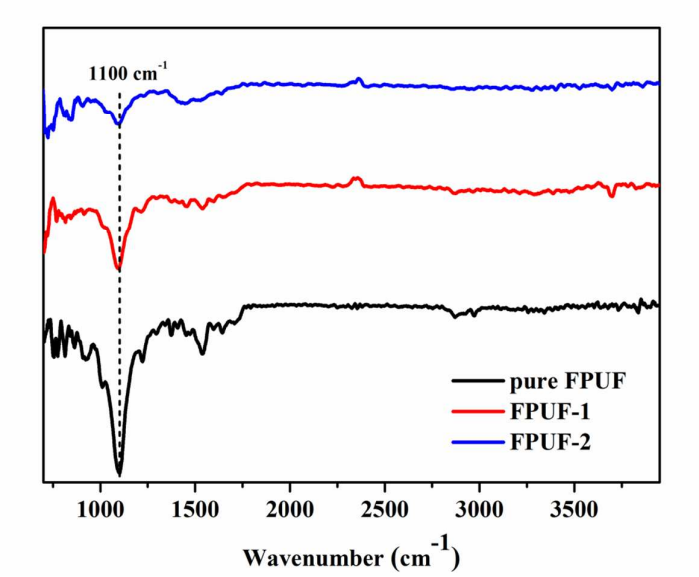

Fig. 2. ATR-FTIR spectra of pure and coated FPUF.

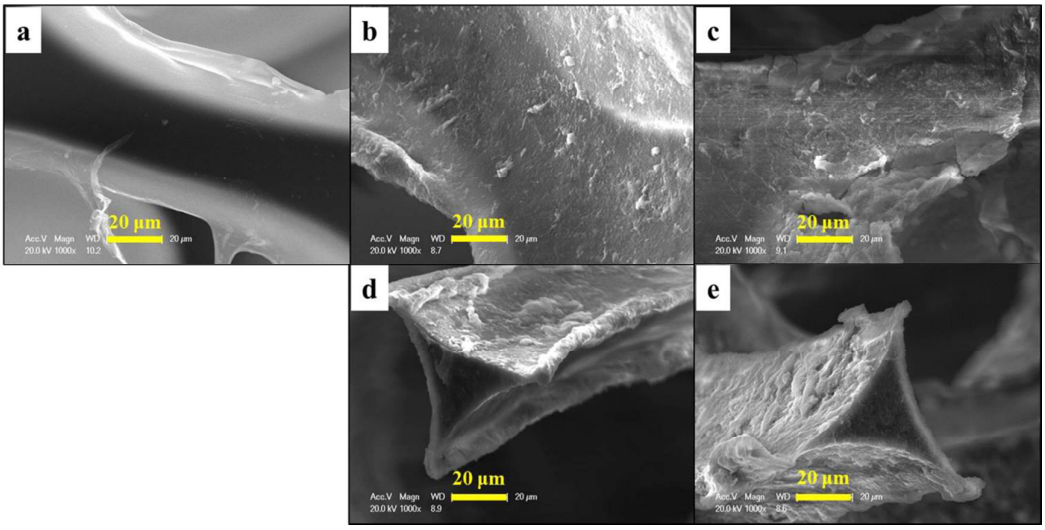

Fig. 3. SEM images of pure FPUF (a), FPUF-1 (b, d) and FPUF-2 (c, e).

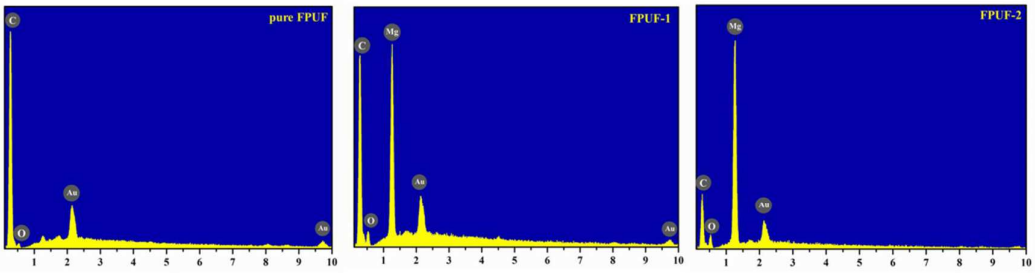

Fig. 4. EDX spectra of the pure FPUF, FPUF-1 and FPUF-2.

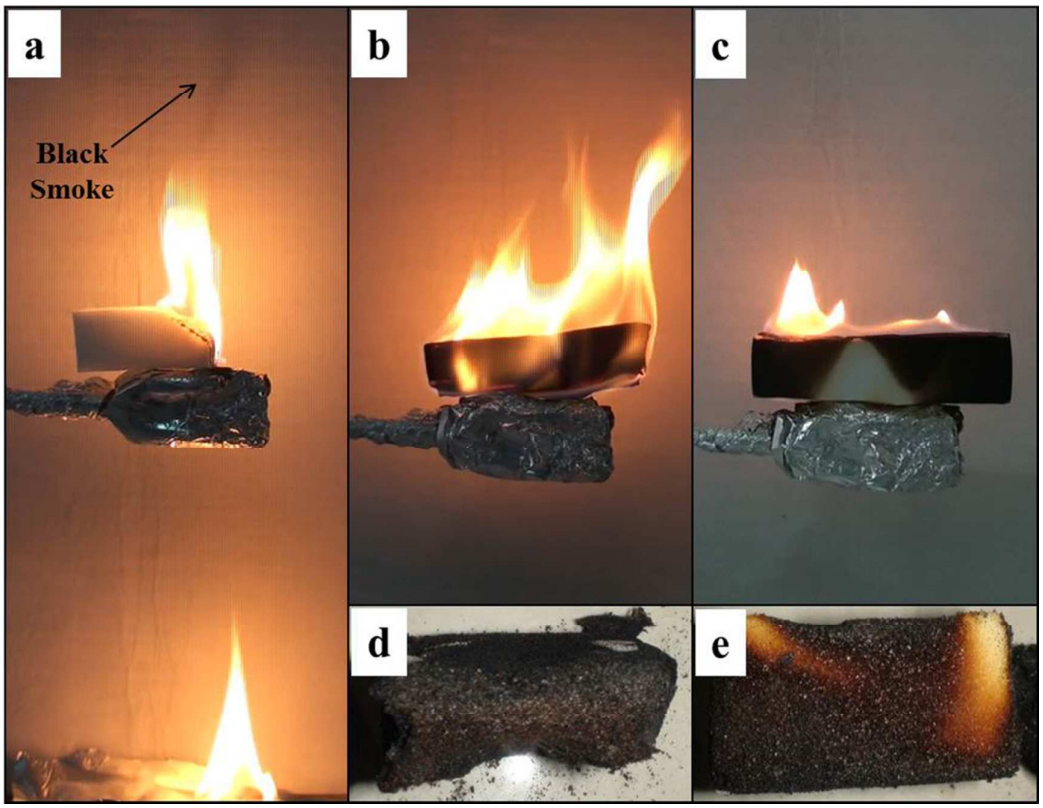

Fig. 5. Photographs of 40s after ignition by holding the flame from a butane torch on the surfaces of pure FPUF (a), FPUF-1 (b) and FPUF-2 (c) for 10 s. Cross section images of FPUF-1 (d) and FPUF-2 (c)'s char residues after burning.

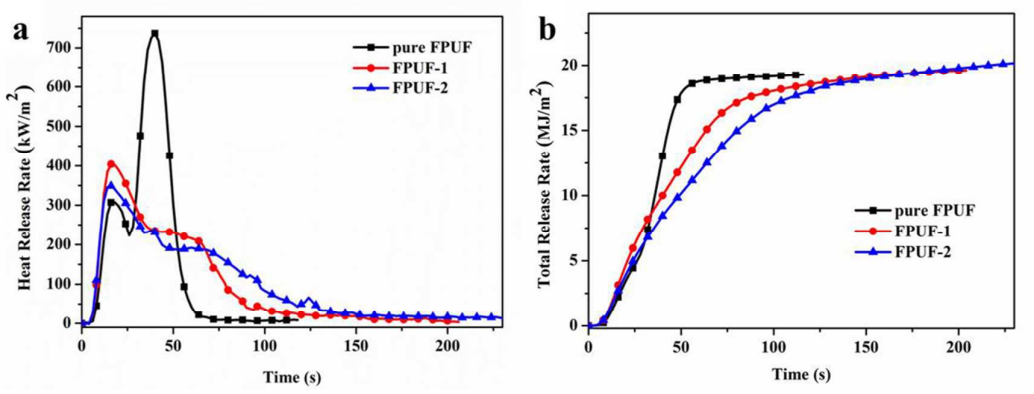

Fig. 6. Heat release rate (a) and total heat release (b) curves of pure and coated FPUFs.

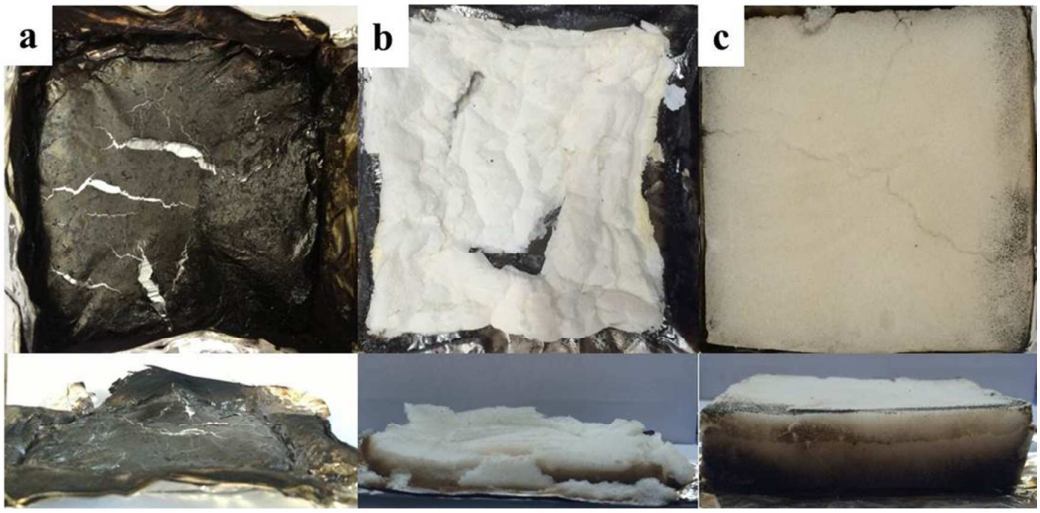

Fig. 7. Photographs of pure FPUF (a), FPUF-1 (b) and FPUF-2 (c) after cone calorimeter.

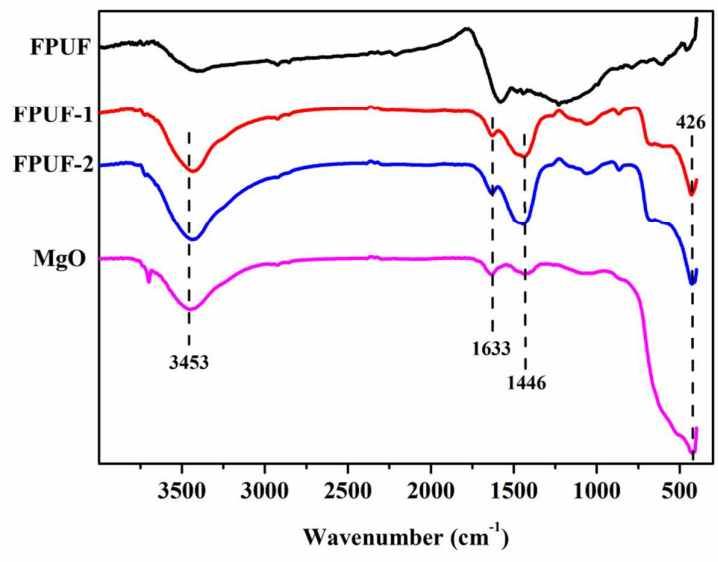

Fig. 8. FTIR curves of uncoated and coated FPUFs' char residue after CONE and MgO.

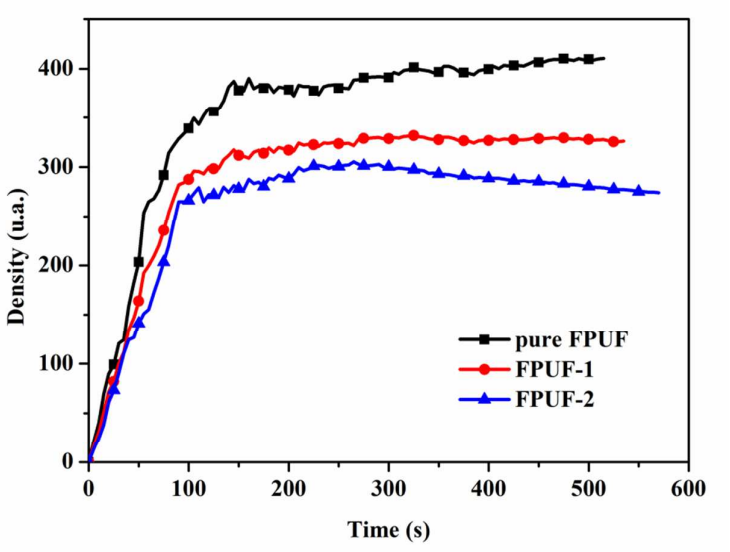

Fig. 9. Released smoke density of pure FPUF, FPUF-1 and FPUF-2 while burning under 25kW m^{-2} heat flux.

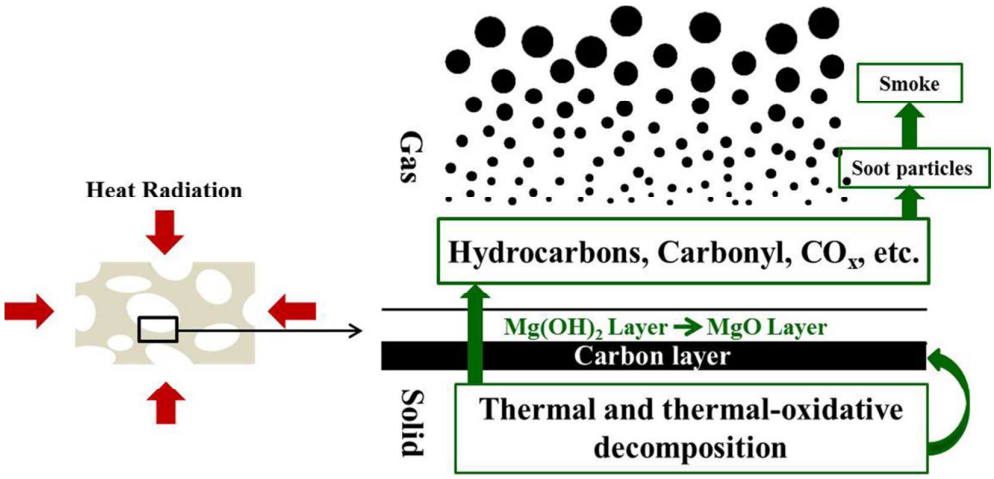

Fig. 10. Model of smoke generation from the burning coated FPUF.

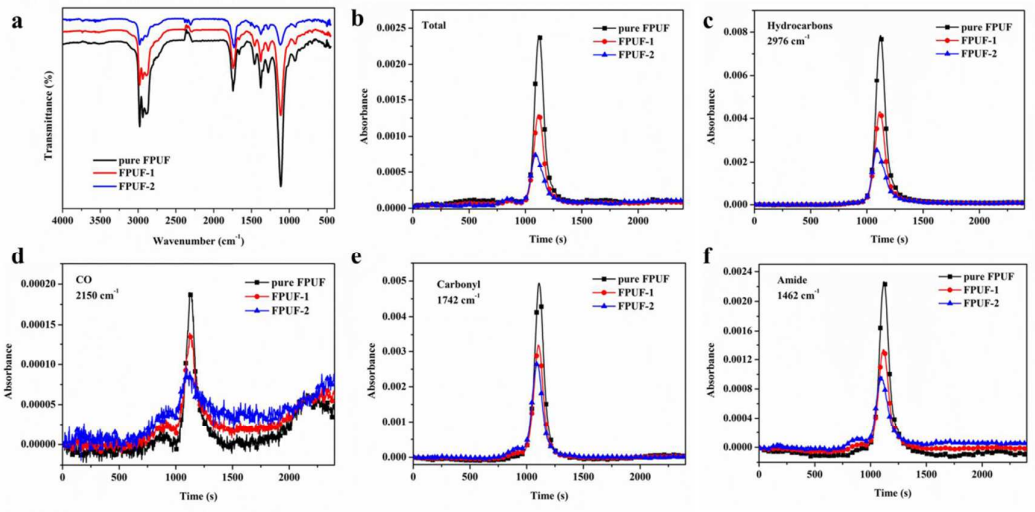

Fig. 11. FTIR spectra of volatilized pyrolysis product emitted from pure FPUF, FPUF-1 and FPUF-2 at maximum evolution rate (a). Absorbance of pyrolysis products for pure FPUF, FPUF-1 and FPUF-2 vs time: (b) Total; (c) Hydrocarbons; (d) CO; (e) Carbonyl and (f) amide.

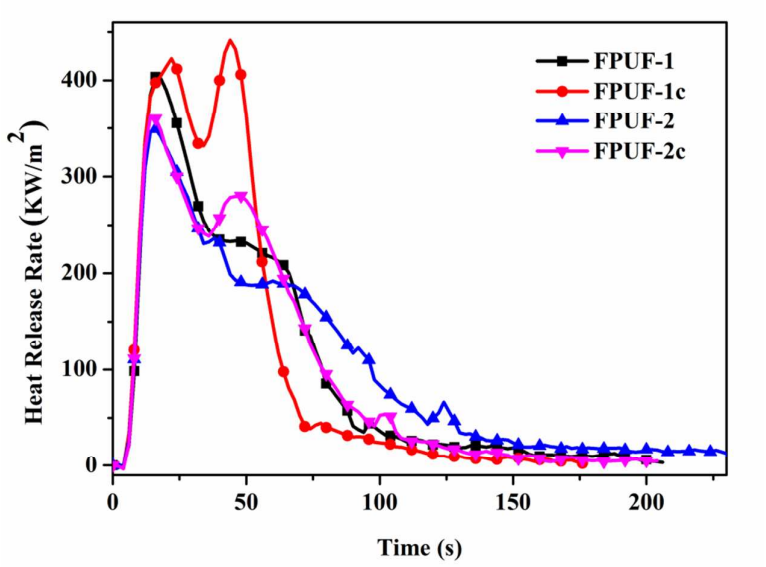

Fig. 12. Heat release rate curves of coated FPUF (FPUF-1 and FPUF-2) and coated FPUF after compression (FPUF-1c and FPUF-2c).